

A crystalline-orientation self-selected linearly polarized Yb:Y3Al5O12 microchip laser

Jun Dong, Akira Shirakawa, and Ken-ichi Ueda

Citation: *Appl. Phys. Lett.* **93**, 101105 (2008); doi: 10.1063/1.2980423

View online: <http://dx.doi.org/10.1063/1.2980423>

View Table of Contents: <http://apl.aip.org/resource/1/APPLAB/v93/i10>

Published by the [American Institute of Physics](#).

Related Articles

Note: Self Q-switched Nd:YVO4 laser at 914 nm

Rev. Sci. Instrum. **83**, 046110 (2012)

Stable dual-wavelength microlaser controlled by the output mirror tilt angle

Appl. Phys. Lett. **99**, 241113 (2011)

Continuous-wave cascaded-harmonic generation and multi-photon Raman lasing in lithium niobate whispering-gallery resonators

Appl. Phys. Lett. **99**, 221111 (2011)

Thermal, spectroscopic, and laser characterization of Nd:LuxY1-xVO4 series crystals

AIP Advances **1**, 042143 (2011)

Efficient continuous wave deep ultraviolet Pr³⁺:LiYF₄ laser at 261.3nm

Appl. Phys. Lett. **99**, 181103 (2011)

Additional information on *Appl. Phys. Lett.*


Journal Homepage: <http://apl.aip.org/>

Journal Information: http://apl.aip.org/about/about_the_journal

Top downloads: http://apl.aip.org/features/most_downloaded

Information for Authors: <http://apl.aip.org/authors>

ADVERTISEMENT

INSTRUMENTS FOR ADVANCED SCIENCE			
	Gas Analysis dynamic measurement of reaction gas streams catalysis and thermal analysis molecular beam studies dissolved species probes fermentation, environmental and ecological studies	Surface Science UHV TPD SIMS end point detection in ion beam etch elemental imaging - surface mapping	Plasma Diagnostics plasma source characterisation etch and deposition process reaction kinetic studies analysis of neutral and radical species
	Vacuum Analysis partial pressure measurement and control of process gases reactive sputter process control vacuum diagnostics vacuum coating process monitoring		
contact Hiden Analytical for further details: info@hiden.co.uk www.HidenAnalytical.com CLICK TO VIEW OUR PRODUCT CATALOGUE			

A crystalline-orientation self-selected linearly polarized Yb:Y₃Al₅O₁₂ microchip laser

Jun Dong,^{a)} Akira Shirakawa, and Ken-ichi Ueda

Institute for Laser Science, University of Electro-Communications, 1-5-1 Chofugaoka, Chofu, Tokyo 182-8585, Japan

(Received 2 June 2008; accepted 20 August 2008; published online 9 September 2008)

Crystalline-orientation and pump dependent polarization states of Yb:Y₃Al₅O₁₂ microchip lasers were observed experimentally. Linear polarization was observed at six crystalline orientations in the (111) plane relative to the beam propagation direction along the [111] crystalline axis of Yb:Y₃Al₅O₁₂ crystal. The extinction ratio of the linear polarization decreases and the laser tends to oscillate at random polarization state at high pump power levels. Linear polarization states of Yb:Y₃Al₅O₁₂ microchip laser was selected by the anisotropic spectroscopic properties of the Yb³⁺-ion in cubic Y₃Al₅O₁₂ crystal. The random polarization oscillation at high pump power was caused by the strong thermal-induced birefringence and depolarization. © 2008 American Institute of Physics. [DOI: 10.1063/1.2980423]

Well-polarized laser sources have various applications in optical systems, such as nonlinear frequency conversion,¹ polarization-coupled laser beam combining, interferometers, semiconductor optical amplifiers, and optical modulators, which have polarization-dependent properties. Polarized solid-state lasers are usually achieved by using polarization-dependent anisotropic laser crystals (e.g., Nd:vanadate² or Nd:yttrium lithium fluoride³) or intracavity polarizing elements such as a Brewster's window, with linearly polarized longitudinal pumping or using polarized feedback and so on. Rare-earth ion doped Y₃Al₅O₁₂ [yttrium aluminum garnet (YAG)] lasers have been extensively exploited for many applications because the YAG host has excellent thermal, chemical, and mechanical properties.⁴ Recently, Yb:YAG has been demonstrated to be a promising candidate for high-power laser-diode pumped solid-state lasers.⁵ In Yb:YAG crystal, Yb³⁺ substitutes Y³⁺ on the dodecahedral sites, which are not cubic, it is *D*₂ symmetry. There are six crystallographically equivalent but orientation inequivalent sites in the Yb:YAG crystal. The Yb³⁺ ions should show well-polarized spectra in the local symmetry axes; however, the overall symmetry of the garnets is cubic, giving rise to completely unpolarized spectra for the Yb:YAG crystal. The crystal-field investigation for Tb:YAG,⁶ Eu:YAG,⁷ and Er:Yb:YAG (Ref. 8) crystals by site-selective polarized spectroscopy and polarization dependence of the site-selectively excited fluorescence of Ho:YAG (Ref. 9) shows that the symmetry of rare-earth ions in *D*₂ site is lowered, it was suggested that it is lowered to the trigonal system, space group *R*3.¹⁰ Also, orientation dependent saturation absorption of Cr⁴⁺:YAG crystal has been observed under different high intensity light at 1.064 μm.¹¹ Although there are some reports on polarization states of single-mode Nd:YAG lasers, the Nd:YAG crystal is assumed to be optically pumped longitudinally with a laser of specified polarization.¹² The anisotropic (100)-cut Nd:YAG crystal was used as gain me-

dium to obtain polarized mode oscillation recently.¹³ The commonly commercial available Nd:YAG or Yb:YAG crystals are usually grown along the [111] direction. The propagation of YAG lasers is along the [111] direction, and the polarized states of these lasers are usually achieved by adopting external forces such as stress and temperature. Until now, there have been no reports on crystalline orientation selected polarized lasers from cubic YAG doped with rare-earth ions when the light propagates along the [111] crystal growth axis. We now present the first experimental demonstration of a linearly polarized continuous-wave microchip laser based on cubic Yb:YAG crystal selected by the crystalline orientations in the (111) plane when the light propagates along the [111] direction. The effect of pump power induced birefringence and depolarization on the crystalline orientation selected linearly polarized states of continuous-wave Yb:YAG microchip lasers was addressed.

A schematic diagram of experimental setup for crystalline-orientation selected polarization states of microchip Yb:YAG lasers is shown in Fig. 1. 1-mm-thick plane-parallel Yb:YAG single crystal plates (*C*_{Yb}=10, 15, and 20 at. %) were used as gain media. Yb:YAG crystals were grown by Czochralski method along the [111] direction. One surface of the Yb:YAG plate perpendicular to the [111] crystalline axis is antireflection coated at 940 nm and high reflection coated at 1030 nm to act as a cavity mirror of the laser. The other surface of the Yb:YAG is antireflection coated at 1030 nm to reduce the cavity loss. Plane-parallel mirrors were used as output couplers with different transmissions (*T*_{oc}) of 5% and 10% at 1.03 μm. The Yb:YAG crystal and

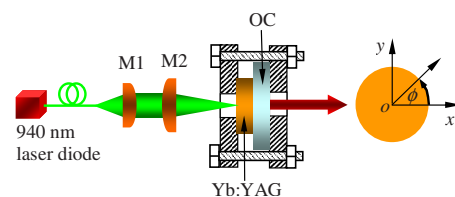


FIG. 1. (Color online) Schematic diagram for measurement of polarization of continuous-wave Yb:YAG microchip laser. M1 and M2 are the focus lenses, OC, is the output coupler, and ϕ is crystal rotation angle.

^{a)} Author to whom correspondence should be addressed. Present address: Department of Physics, School of Engineering and Physical Sciences, Heriot-Watt University, Edinburgh EH14 4AS, UK. Electronic mail: jundong_99@yahoo.com.

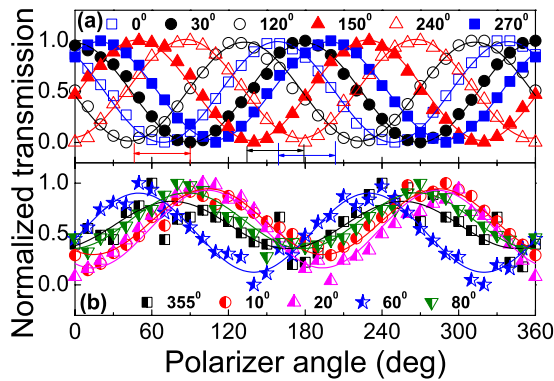


FIG. 2. (Color online) (a) Linear polarization of continuous-wave Yb:YAG microchip laser as a function of polarizer angle for six different rotation angles along the [111] direction of Yb:YAG crystal. (b) Polarization states as a function of polarizer angle for the rotation angles of Yb:YAG along the [111] direction except from the six angles in Fig. 2(a). The symbols show the experimental data, and the solid lines show the sine fitting.

output coupler were held together with a copper holder, which can be rotated around the axis of laser propagation direction. The Yb:YAG sample is rotated counterclockwise. A fiber-coupled 940 nm laser-diode with a core diameter of 100 μm and numerical aperture of 0.22 was used as the pump source. Two lenses of 8 mm (M1) and 12 mm (M2) focal length were used to focus the pump beam on the crystal rear surface and to produce a pump light footprint in the crystal of about 120 μm in diameter. The Yb:YAG laser was operated at room temperature without active cooling of the active element. The polarization states of these microchip lasers were determined by using a Glan–Thomson prism and a power meter.

To fully understand the nature of orientation inequivalent Yb^{3+} ions in crystallographically equivalent cubic YAG crystals on the polarization states of Yb:YAG microchip lasers, the polarization state of the pump beam used in the experiment is instantaneously random polarization. Therefore, the effect of linearly polarized pump light on the polarization states of Yb:YAG microchip lasers was eliminated. The crystalline-orientation selected polarization states of Yb:YAG microchip lasers were obtained by measuring the output power after the polarizer. Linear polarization states of Yb:YAG microchip lasers were observed when the absorbed pump power intensity was lower than 45 kW/cm^2 . Figure 2 shows the normalized transmission of Yb:YAG microchip lasers after polarizer as a function of polarizer angle for different rotation angles of Yb:YAG crystals along the [111] direction when the absorbed pump power intensity was 20 kW/cm^2 . Six orientations in the (111) plane, which are perpendicular to the laser emitting direction [111] exhibit “perfect” linear polarization (extinction ratio >100) of the continuous-wave output power of Yb:YAG microchip lasers, as shown in Fig. 2(a). 0° indicates the first position that has perfect linear polarization when the Yb:YAG sample was rotated anticlockwise. Then the sample was continuously rotated along the same direction, and there are another five positions (30°, 120°, 150°, 240°, and 270° away from the first linearly polarized position) exhibiting linear polarization. A total of six positions exhibiting perfect linear polarization were found. When the rotating angle was set between any two of these six positions, although Yb:YAG continuous-wave microchip lasers still exhibit the linear polarization in

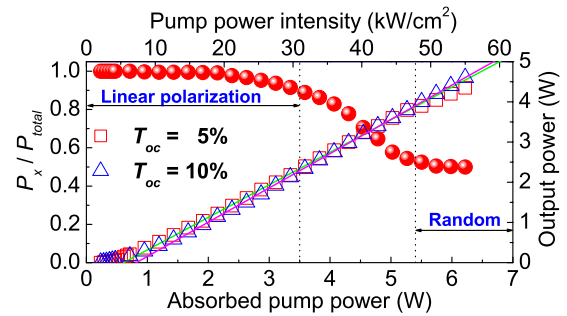


FIG. 3. (Color online) Output power (1049 nm oscillation for $T_{oc}=5\%$ and 1030 nm oscillation for $T_{oc}=10\%$) and ratio of the horizontal polarized component to the total output power P_x/P_{total} , as a function of the absorbed pump power.

some degrees, the variation of the output power does not show clearly perfect linear polarization, some examples are shown in Fig. 2(b). Figure 3 shows the output power and the ratio of the horizontal polarized component to the total output power of six crystalline-orientation selected polarized lasers as a function of the absorbed pump power. Best laser performance at 1030 and 1049 nm was achieved with 10 at. % Yb:YAG crystal for different output couplings.¹⁴ Maximum output power of 4.6 W was measured for $T_{oc} = 10\%$ when the absorbed pump power was 6.2 W. The slope efficiency is about 85% and optical-to-optical efficiency is about 74%. The laser polarization states of continuous-wave Yb:YAG microchip lasers were strongly affected by the absorbed pump power. The laser exhibits a linear polarization state at low absorbed pump power, and the extinction ratio of linear polarization decreases with increase of the absorbed pump power intensity (between 30 and 45 kW/cm^2). The laser oscillates with random polarization states at higher pump power intensity (>45 kW/cm^2).

Crystalline-orientation self-selected polarization states of Yb:YAG microchip lasers at low pump power levels are caused by the threefold local symmetry of dodecahedral coordinated Yb^{3+} ions in cubic YAG crystal. Figure 4(a) shows the six possible orientations of cubic YAG doped with Yb^{3+} ions and their relationship to the axes XYZ of the unit cell, preferable for linear polarization oscillation. The local axes x_i are parallel to the cubic axes of the unit cell, while the axis y_i and z_i are parallel to the face diagonals. There are three local sites in Yb:YAG crystal. Each site includes two orien-

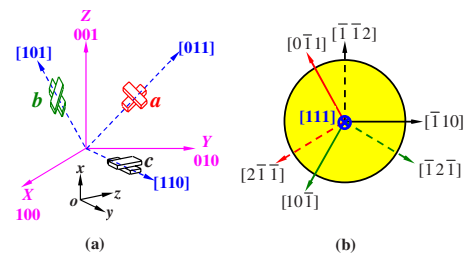


FIG. 4. (Color online) The Yb^{3+} substitution sites in the YAG matrix, the crystal cell axes are denoted [100], [010], and [001]. (a) Crystalline-orientation of the three inequivalent sites of the Yb^{3+} ion in the cubic YAG relative to the axes XYZ of the cubic unit cell. The edges of the right parallelepipeds indicate the orientation of the local twofold axes x_i, y_i, z_i in the order of growth length. The oy axis coincides with the crystal cell diagonal [110]. In each site, the transition dipole moment, represented by an oblong, is directed along the local oy axis. (b) The six polarization-preferable orientations in the (111) plane.

tations that are perpendicular to each other, such as $[\bar{1}10]$ and $[\bar{1}\bar{1}2]$, $[0\bar{1}1]$ and $[2\bar{1}\bar{1}]$, and $[10\bar{1}]$ and $[\bar{1}2\bar{1}]$. All these orientations are in the (111) plane and are perpendicular to the $[111]$ direction. The relative positions of these six orientations in the (111) plane are shown in Fig. 4(b). Under the random polarization pumping, all sites are excited equally; therefore, gain is the same for both cavity polarized lasing modes. In the case of linearly polarized light, the lasing gain is proportional to $\cos^2(\alpha_a)n_a + \cos^2(\alpha_b)n_b + \cos^2(\alpha_c)n_c$, where n_i are the inversion population of the sites a , b , and c , and α_i are the angles of the local sites x_i with regard to the laser electric field E . The Yb:YAG microchip lasers oscillate along the $[111]$ direction. The laser electric field E must therefore lie in a plane perpendicular to the $[111]$ direction. Assume for simplicity that the laser is oriented in such a way that its eigenpolarizations are along $[\bar{1}10]$ and $[\bar{1}\bar{1}2]$ directions. For the $[\bar{1}10]$ polarization, the gain is proportional to $(\frac{1}{2}n_a + \frac{1}{2}n_b)$, and for the $[\bar{1}\bar{1}2]$ polarization, it is proportional to $(\frac{1}{6}n_a + \frac{1}{6}n_b + \frac{4}{6}n_c)$. The laser cavity polarization develops first depending on the initial fluctuations in spontaneous noise. In a case when the laser is polarized along $[\bar{1}10]$ direction, only populations of the sites a and b are depleted during the laser oscillation. When the Yb:YAG crystal was rotated anticlockwise, the combined gain for the linear polarization provided from three sites was changed accordingly, therefore, the laser cavity polarization was changed away for $[\bar{1}10]$ direction. Further rotating Yb:YAG crystal until the laser cavity polarization along $[\bar{1}\bar{1}2]$ direction, populations from sites a , b , and c contributed to the laser oscillation. Similar arguments can be made for any orientation of the cavity laser polarization modes with regard to the crystal axes. These orientations $\langle\bar{1}10\rangle$ and $\langle\bar{1}\bar{1}2\rangle$ in the (111) plane are preferable for polarized light propagation when the intracavity polarization is along these orientations, therefore, crystalline-orientation selected linearly polarized laser was observed in microchip lasers. When the crystal was rotated at the positions between any two of these six specified orientations, two linearly polarized modes can get enough gain provided from three sites, two polarized modes oscillate unevenly and simultaneously, therefore, less perfect linearly polarized light was observed in the experiments [as shown in Fig. 2(b)]. At substantially higher absorbed pump powers, the pump power induced photoelastic effect applied, perturbing the cubic structure of the Yb:YAG crystal so that the population inversion becomes less sensitive to the orientations of the crystal. Two polarized modes compete each other and can obtain sufficient gain to oscillate simultaneously. It has been shown in (111)-cut Nd:YAG crystal that depolarization cannot be minimized by rotating the gain crystal to particular angles.¹⁵ The depolarization is usually attributed to the thermal stresses arising from the absorbed pump power in the gain medium. We calculated the depolarization¹⁵ of

our Yb:YAG microchip lasers as a function of the absorbed pump power and found that the depolarization of Yb:YAG microchip lasers increases with absorbed pump power. Moreover, a slope of 0.0042/ W when the absorbed pump power is over 3.5 W, is about three times higher than a slope of 0.0015/ W when the absorbed power is below 3.5 W. The strong depolarization at high pump power affect the polarization states of Yb:YAG microchip lasers and lasers tend to oscillate at random polarization states (as shown in Fig. 3).

In conclusion, crystalline-orientation and pump dependent linear polarization states of laser-diode pumped Yb:YAG microchip lasers were observed. Linear polarization was observed at six crystalline orientations relative to the beam propagation direction along the $[111]$ crystalline axis of Yb:YAG crystal at low pump power range ($<45 \text{ kW/cm}^2$). The extinction ratio of the linear polarization decreases with increase of the pump power intensity and lasers tend to be in random polarization states at high pump power intensity. The crystalline-orientation selected polarization states of continuous-wave Yb:YAG microchip lasers were attributed to the anisotropic symmetry of the Yb^{3+} ions in cubic Yb:YAG crystal. The strong thermal birefringence and depolarization at high pump power level limit the linear polarization of Yb:YAG microchip lasers and the lasers oscillate at random polarization states.

This work was supported by the 21st Century Center of Excellence (COE) program of Ministry of Education, Science, Sports and Culture of Japan.

- ¹A. V. Kir'yanov, V. Aboites, and I. V. Mel'nikov, *J. Opt. Soc. Am. B* **17**, 1657 (2000).
- ²A. W. Tucker, M. Birnbaum, C. L. Fincher, and J. W. Erler, *J. Appl. Phys.* **48**, 4907 (1977).
- ³T. M. Pollak, W. F. Wing, R. J. Grasso, E. P. Chicklis, and H. P. Jenssen, *IEEE J. Quantum Electron.* **18**, 159 (1982).
- ⁴G. A. Bogomolova, D. N. Vylegzhanin, and A. A. Kaminskii, *Sov. Phys. JETP* **42**, 440 (1976).
- ⁵A. Giesen, H. Hugel, A. Voss, K. Wittig, U. Brauch, and H. Opower, *Appl. Phys. B: Lasers Opt.* **58**, 365 (1994).
- ⁶R. Bayerer, J. Heber, and D. Mateika, *Z. Phys. B: Condens. Matter* **64**, 201 (1986).
- ⁷H. Gross, J. Neukum, J. Heber, D. Mateika, and T. Xiao, *Phys. Rev. B* **48**, 9246 (1993).
- ⁸L. Dobrzycki, E. Bulska, D. A. Pawlak, Z. Frukacz, and K. Wozniak, *Inorg. Chem.* **43**, 7656 (2004).
- ⁹M. D. Seltzer, M. E. Hills, and J. B. Gruber, *Phys. Rev. B* **46**, 8007 (1992).
- ¹⁰J. Chenevas, J. C. Joubert, M. Marezio, and B. Ferrand, *J. Less-Common Met.* **62**, 373 (1978).
- ¹¹H. Eilers, K. R. Hoffman, W. M. Dennis, S. M. Jacobsen, and W. M. Yen, *Appl. Phys. Lett.* **61**, 2958 (1992).
- ¹²R. Dalgliesh, A. D. May, and G. Stephan, *IEEE J. Quantum Electron.* **34**, 1485 (1998).
- ¹³A. McKay, J. M. Dawes, and J. Park, *Opt. Express* **15**, 16342 (2007).
- ¹⁴J. Dong, A. Shirakawa, K. Ueda, and A. A. Kaminskii, *Appl. Phys. B: Lasers Opt.* **89**, 359 (2007).
- ¹⁵T. Shoji and T. Taira, *Appl. Phys. Lett.* **80**, 3048 (2002).